

8×10^{-17} fractional laser frequency instability with a long room-temperature cavity

Sebastian Häfner,¹ Stephan Falke,^{1,3} Christian Grebing,¹ Stefan Vogt,¹ Thomas Legero,¹
Mikko Merimaa,² Christian Lisdat,¹ and Uwe Sterr^{1,*}

¹Physikalisch-Technische Bundesanstalt (PTB), Bundesallee 100, 38116 Braunschweig, Germany

²VTT Technical Research Centre of Finland Ltd Centre for Metrology MIKES, P.O. Box 1000, FI-02044 VTT Espoo, Finland

³TOPTICA Photonics AG, Lochhamer Schlag 19, 82166 Gräfelfing, Germany

*Corresponding author: uwe.sterr@ptb.de

Received February 4, 2015; revised March 25, 2015; accepted March 30, 2015;
posted April 1, 2015 (Doc. ID 233886); published May 1, 2015

We present a laser system based on a 48 cm long optical glass resonator. The large size requires a sophisticated thermal control and optimized mounting design. A self-balancing mounting was essential to reliably reach sensitivities to acceleration of below $\Delta\nu/\nu < 2 \times 10^{-10}/g$ in all directions. Furthermore, fiber noise cancellations from a common reference point near the laser diode to the cavity mirror and to additional user points (Sr clock and frequency comb) are implemented. Through comparison with other cavity-stabilized lasers and with a strontium lattice clock, instability of below 1×10^{-16} at averaging times from 1 to 1000 s is revealed. © 2015 Optical Society of America

OCIS codes: (140.4780) Optical resonators; (140.3425) Laser stabilization; (120.3940) Metrology.
<http://dx.doi.org/10.1364/OL.40.002112>

Lasers with high frequency stability are urgently needed in various fields of physics and technology, e.g., for precision measurements, for the operation of optical clocks [1,2], or for the generation of low-phase-noise microwave signals [3]. The stability of today's best optical clocks [4] is limited by laser frequency noise due to the Dick effect [5]. While alternative concepts for laser frequency stabilization like spectral hole burning [6], or active atomic clocks [7], are currently under investigation, most ultra-stable lasers are based on well-isolated resonators. The best present room temperature resonators provide fractional laser instabilities of 1×10^{-16} – 2×10^{-16} [8,9], limited by thermal Brownian noise from their constituents [10], with the biggest contributions from mirror coatings. This noise can be reduced by operation at cryogenic temperatures [11], increasing the mode size [12], or using a longer cavity [9].

Here we employ the last approach and report on the design and evaluation of a 48 cm long room temperature resonator with a spacer made from ultralow-expansion glass (ULE). Compared with a cryogenic cavity, we can operate the system at ambient temperatures directly at the Sr lattice clock 698 nm transition [13], which simplifies the system and its operation. However, the use of long cylindrical and heavier cavities makes it much more difficult to reach the required suppression of optical length changes through forces induced by seismic vibrations and through thermal expansion caused by temperature fluctuations. In the following text, we describe the vibration insensitive mounting, temperature control, optical setup, and fiber noise cancellation system.

We use a cylindrical ULE-glass spacer of 48 cm length and 9 cm diameter. With two optically contacted fused silica mirrors (one plane mirror and the other one with radius of curvature $R = 1$ m) we expect a thermal noise level [14] of 5.4×10^{-17} . The system provides a cavity finesse of $F = 282,000$ (1.1 kHz linewidth) as measured from the optical ring down. Before the final optical contact, finesse was optimized by moving the mirrors to

minimize the influence of coating defects. ULE rings are attached to the rear sides of both mirrors to avoid the effect of the differential thermal expansion between the fused silica substrate and the ULE-glass spacer [15]. The resonator is held horizontally on four points (Fig. 1) in small cutouts (length 40 mm, depth 4 mm) machined to the sides of the spacer [16–18]. Accelerations acting on the resonator due to seismic noise both change the cavity length L_{geo} between the nominal centers of the mirrors (geometrical axis) and lead to tilts of the mirrors through bending of the spacer. Mirror tilt leads to a change in the optical length if there is a mismatch between the geometrical axis and the optical axis. The high symmetry of the resonator and the mount largely suppresses the sensitivity of L_{geo} to accelerations in y and z directions. In addition, the positions and dimensions of the cutouts were optimized by finite-element modeling to minimize

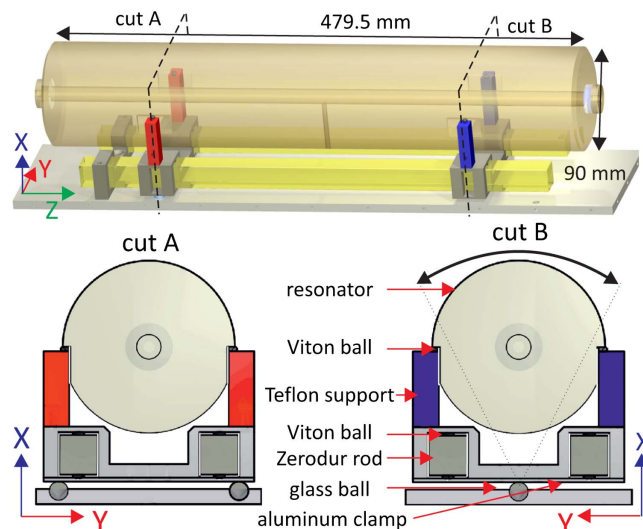


Fig. 1. Resonator mounting design. The lower figures show cuts through the fixed (A) and rotatable (B) supports.

bending and the sensitivity along x . For a long and heavy spacer ($m = 6.8$ kg) as used here, the symmetry of the reaction forces along the optical axis (z) as well in the transverse horizontal direction (y) becomes more important, as already a force difference of 100 nN between the mounting points (along z) leads to a relative length change of 1.3×10^{-16} . Assuming a typical vibration noise of $1 \mu\text{g}$ ($1g = 9.8 \text{ m/s}^2$), these reaction forces need to be balanced on a level of 10^{-3} to reach a fractional instability of below 10^{-16} . The elasticity at all four mounting positions has to be matched very accurately in order to obtain this level of balance of forces.

In our design, the cavity is sitting on four Viton balls (diameter 4 mm), which are placed on top of four Teflon posts. Through height imperfections of the posts, the Viton pieces get compressed differently and the shearing elasticity differs. Thus, the requirements given above are violated. To remove the height imperfections and to realize an effective three-point mount, a self-balancing mount is employed (Fig. 1). Near one end of the resonator (cut B), the two Teflon posts supporting the resonator are mounted on an aluminum clamp on top of a single glass sphere, allowing the structure to rotate around z axis. On the other end (cut A), rotation of the structure around z axis is prevented by two glass spheres underneath the clamp. Thus, the four posts are automatically leveled and the forces at the support points are equalized by this movement of the whole cavity.

To isolate the mounting structure from the thermal expansion of the aluminum base plate, two Zerodur glass rods are inserted between the clamp and the base plate (Fig. 1). Viton balls between the clamps and the glass rods ensure a strong friction force to prevent any horizontal movement of the clamps, while providing the necessary flexibility for the balanced mount. By experimentally varying the distance between the Viton balls that hold the resonator, the vibration sensitivities κ_i were optimized to $\kappa_z = 1.7 \times 10^{-10}/\text{g}$, $\kappa_y = 0.5 \times 10^{-10}/\text{g}$, and $\kappa_x = 1.5 \times 10^{-10}/\text{g}$, all measured at 0.7 Hz, in contrast to poorly reproducible values around $4 \times 10^{-8}/\text{g}$, which were initially obtained without a balanced mount.

We measured the thermal expansion coefficient α of the resonator as $\alpha(T) = 2 \times 10^{-9} \text{ K}^{-2}(T - T_0)$ with a zero-crossing temperature of $T_0 = -0.24^\circ\text{C}$. Thus, if operated within 50 mK of T_0 , a temperature stability of better than $1 \mu\text{K}$ is required to reach a fractional frequency instability of below 10^{-16} . The large dimensions of the setup can easily lead to large temperature gradients that fluctuate with the ambient temperature, which exacerbates the control of the average temperature of the resonator at the required level. To achieve the required stability, we start by stabilizing the temperature of the vacuum chamber by thermoelectric coolers (TECs) close to the ambient temperature.

Inside the vacuum chamber, the temperature of the first heat shield is stabilized at T_0 using TECs mounted between the shield and the chamber. To reduce the influence of thermal gradients on the cavity, this first shield is temperature-stabilized in three sections along the axial direction (z). For each section, a weighted temperature from thermistors at the top and bottom ($\approx 1:5$) of the shield is used as input to a temperature control loop. The relative contributions of the sensors were determined

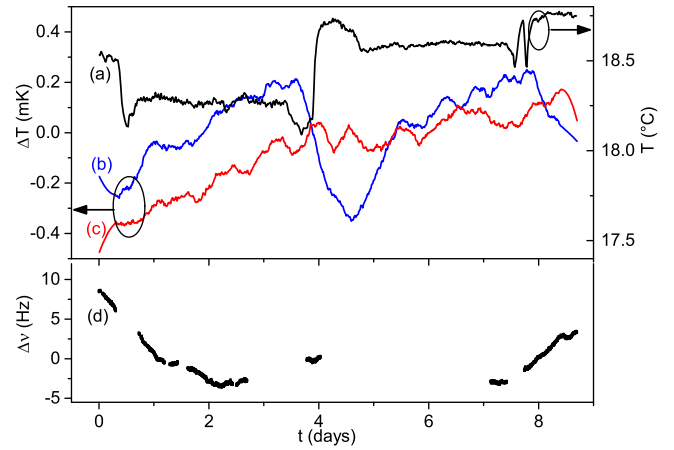


Fig. 2. (a) Temperature in the acoustic isolation box surrounding the vacuum chamber, and temperature fluctuations (b) on the active heat shield and (c) next to the cavity. Plot (d) shows residual cavity frequency fluctuations measured against the Sr reference with a linear drift of 20 mHz/s subtracted.

experimentally by introducing gradients in the vacuum chamber and minimizing the remaining temperature fluctuation of the second shield. Further inside, a third heat shield surrounds the resonator. The polished aluminum heat shields act as low-pass filters for temperature fluctuations with a measured time constant of $\tau_{\text{th}} \approx 8$ d.

With this advanced temperature control, the temperature fluctuations of the outer passive shield remain within $\approx 500 \mu\text{K}$ when the room temperature changes by 0.5 K (Fig. 2). No significant influence was observed at the resonator. After the removal of an average drift of 20 mHz/s due to aging of the spacer material, the frequency of the resonator fluctuates by ± 6 Hz. Assuming an offset of 50 mK of the resonator temperature from T_0 , these frequency deviations correspond to temperature fluctuations of $\pm 120 \mu\text{K}$.

This resonator setup is the central part of the interrogation laser system for a ^{87}Sr optical lattice clock [13]. The frequency of a filter-stabilized 698 nm extended-cavity laser diode [19,20] is locked to the cavity via the Pound-Drever-Hall (PDH) technique [21]. Light is sent through an offset acousto-optic modulator (AOM), which allows tuning the frequency to the ^{87}Sr clock transition, and via a 2 m long optical fiber to the vibration isolation table. There, the light is phase-modulated by a free-space electro-optic modulator (EOM) required for PDH stabilization and then sent through several windows to the resonator. Any reflection from the optical components in the optical path back to the cavity leads to frequency pulling of the cavity resonance. By placing a quarter-wave plate inside the vacuum system directly in front of the cavity mirror, all these reflections have orthogonal polarization with respect to the initial polarization and should not contribute to frequency pulling.

Faraday isolators, 35 dB before and 38 dB behind the EOM, suppress the effects of spurious reflections, which may also produce residual amplitude modulation (RAM). The potential frequency shift due to RAM is of the order of 10^{-17} , thus no active control was implemented. Significant frequency shifts are introduced by the thermal deformation and optical length change caused by light

absorbed in the mirror coatings. It leads to a sensitivity of 120 Hz per μW of power transmitted through the cavity. We send a light power of $35 \mu\text{W}$ to the resonator; about 70% of the carrier is coupled in and $2 \mu\text{W}$ are transmitted. The transmitted power was stabilized with the offset AOM. An out-of-loop measurement of the power instability converts into a frequency instability of below 5×10^{-17} at 1 s averaging time. The instabilities calculated from the shot noise for the transmitted light as well as for the light for the PDH lock are well below 10^{-17} .

The optical path lengths (including the optical fibers) to the reference cavity, to the Sr experiment, and to a frequency comb are all stabilized, using a common reference mirror near the clock laser. Special attention is paid to the optical path between the reference mirror and the cavity. Since it is inside the PDH stabilization loop, any phase noise ϕ_{path} from length fluctuations is added to the laser light at the reference mirror and to the light sent elsewhere. Path length stabilization by retroreflecting light from the cavity back through the fiber [22] is incompatible with the required optical isolation as described above. To circumvent this dilemma, we deliver phase-stable light with an additional noise-canceled fiber using the common reference mirror and superimpose it with the light transmitted through the reference cavity. Phase fluctuations in the heterodyne beat signal originate from ϕ_{path} and are compensated through the offset AOM.

The system performance was evaluated by comparison with a laser locked to a cryogenic silicon cavity at 1542 nm [11] via a frequency comb and a 698 nm transportable laser system based on a 12 cm long ULE cavity with fused silica mirrors. From two simultaneously sampled optical beats between these systems, the spectral power densities of the frequency fluctuations $S_y(f)$ between all three systems were calculated. As these statistical spectral quantities behave the same way as Allan variances σ_y^2 , the individual noise components $S_i(f)$ were computed with the three-cornered hat method [23] [Fig. 3(a)]. For higher Fourier frequencies, the noise was

estimated from the beat between the spectrally filtered light transmitted through the cavity with light coming directly from the laser [Fig. 3(b)]. At high frequencies, this noise approaches the frequency noise of the free-running laser [Fig. 3(c)].

The inset in Fig. 3 shows the acceleration spectrum perturbing the cavity. Frequency features at 1 and 7 Hz from resonances of the passive table can also be identified in the laser spectrum. The laser noise peak at 20 Hz, which is not clearly visible in the vibration spectra, presumably originates from a mechanical resonance of the resonator mounted on the Teflon posts.

The instability of the laser system for averaging times between 100 ms and 10 s was calculated with the three-cornered hat method with the two lasers mentioned above (Fig. 4). Frequency data were taken by three frequency counters over 10 h with a gate time of 100 ms and a single linear drift was subtracted. The data set was cut in over 100 sections and individual Allan deviations were calculated.

The instability from 10 to 2000 s was calculated by analyzing the offset frequency from the Sr transition shown in Fig. 2(d). The data set of about 240,000 s was cut in 10,000 s long sections; a linear drift was removed for each section for compensating for the temperature drift and Allan deviations were calculated. For both methods, the arithmetic means of the deviations are shown in Fig. 4. The measured instability of 8×10^{-17} nearly reaches the calculated thermal noise floor of 5.4×10^{-17} . The outstanding frequency instability of below 1×10^{-16} for averaging times from 1 s up to 1000 s indicates high seismic noise suppression and good thermal control. We assume that the stability at short averaging times is still limited by seismic noise and the free-running laser linewidth in combination with the PDH servo bandwidth of 0.8 MHz.

We have presented to our knowledge the first frequency-stabilized laser setup that shows an instability of below 1×10^{-16} over a wide range of averaging times, close to the thermal noise limit of this 48 cm long cavity. Both the observed flicker floor near the thermal limit and

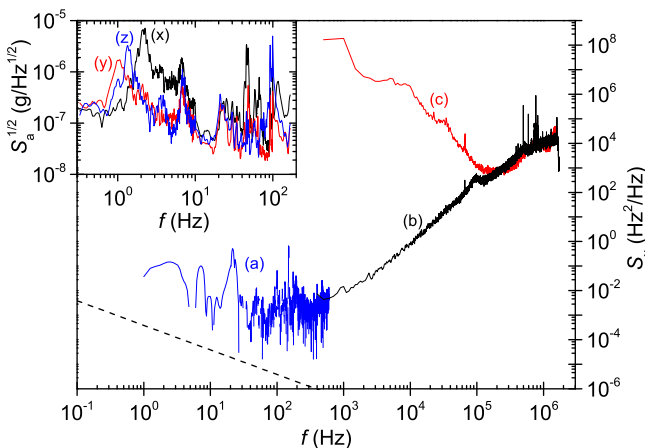


Fig. 3. Noise spectra of (a) the laser locked to the cavity with the three-cornered hat method in the frequency domain, (b) from the light transmitted through the cavity, and (c) of the free-running laser, and the calculated cavity thermal noise (dashed black line). For details see text. The inset displays the power spectral density of acceleration S_a on the passive vibration isolation table close to the cavity, in x , y , z directions.

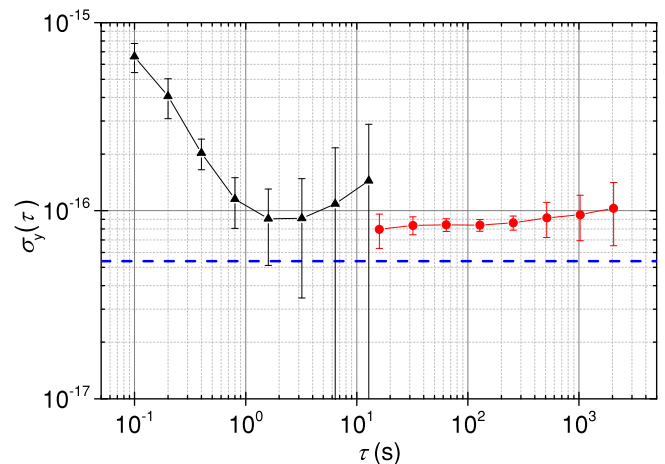


Fig. 4. Allan deviations (overlapping) of the cavity-stabilized laser system from the three-cornered hat method (black solid triangles) and from comparison with the Sr reference (red solid circles) with linear drift removed. The blue dashed line indicates the calculated thermal noise level.

the deviations from a predictable linear drift are comparable to those of cryogenic ($T = 124$ K) single-crystal silicon resonators [14,24]. This was made possible by implementing a novel vibration insensitive mount, temperature control, and optical path length control all the way to the cavity mirror. With laser systems like this, optical clocks will be improved by reducing the Dick effect and by allowing Fourier-limited linewidths for interrogation times beyond one second.

This work was supported by the Centre of Quantum Engineering and Space-Time Research (QUEST), the German Research Foundation (DFG) through RTG 1729 “Fundamentals and applications of ultra-cold matter” and CRC 1128 geo-Q “Relativistic geodesy and gravimetry with quantum sensors,” the European Commission’s FP7 within SOC2, and the European Metrology Research Programme (EMRP) under QESOCAS and ITOC. The EMRP is jointly funded by the EMRP participating countries within EURAMET and the European Union. We thank E. Rasel’s group at LUH for providing the laser and E. Tiemann’s group, from LUH, for providing the ULE-glass spacer, and also thank numerous people from PTB’s mechanical, electronic workshop for help and advice, as well as Ch. Tamm for fruitful discussions.

References

1. T. Rosenband, D. B. Hume, P. O. Schmidt, C. W. Chou, A. Brusch, L. Lorini, W. H. Oskay, R. E. Drullinger, T. M. Fortier, J. E. Stalnaker, S. A. Diddams, W. C. Swann, N. R. Newbury, W. M. Itano, D. J. Wineland, and J. C. Bergquist, *Science* **319**, 1808 (2008).
2. I. Ushijima, M. Takamoto, M. Das, T. Ohkubo, and H. Katori, *Nat. Photonics* **9**, 185 (2015).
3. A. Bartels, S. A. Diddams, C. W. Oates, G. Wilpers, J. C. Bergquist, W. H. Oskay, and L. Hollberg, *Opt. Lett.* **30**, 667 (2005).
4. N. Hinkley, J. A. Sherman, N. B. Phillips, M. Schioppa, N. D. Lemke, K. Beloy, M. Pizzocaro, C. W. Oates, and A. D. Ludlow, *Science* **341**, 1215 (2013).
5. G. J. Dick, “Local oscillator induced instabilities in trapped ion frequency standards,” in *Proceedings of 19th Annual Precise Time and Time Interval Meeting*, Redondo Beach, CA, 1987 (U.S. Naval Observatory, 1988), pp. 133–147.
6. M. J. Thorpe, L. Rippe, T. M. Fortier, M. S. Kirchner, and T. Rosenband, *Nat. Photonics* **5**, 688 (2011).
7. D. Meiser, J. Ye, D. R. Carlson, and M. J. Holland, *Phys. Rev. Lett.* **102**, 163601 (2009).
8. T. Nicholson, M. Martin, J. Williams, B. Bloom, M. Bishof, M. Swallows, S. Campbell, and J. Ye, *Phys. Rev. Lett.* **109**, 230801 (2012).
9. Y. Y. Jiang, A. D. Ludlow, N. D. Lemke, R. W. Fox, J. A. Sherman, L.-S. Ma, and C. W. Oates, *Nat. Photonics* **5**, 158 (2011).
10. K. Numata, A. Kemery, and J. Camp, *Phys. Rev. Lett.* **93**, 250602 (2004).
11. T. Kessler, C. Hagemann, C. Grebing, T. Legero, U. Sterr, F. Riehle, M. J. Martin, L. Chen, and J. Ye, *Nat. Photonics* **6**, 687 (2012).
12. S. Amairi, T. Legero, T. Kessler, U. Sterr, J. B. Wübbena, O. Mandel, and P. O. Schmidt, *Appl. Phys. B* **113**, 233 (2013).
13. S. Falke, N. Lemke, C. Grebing, B. Lipphardt, S. Weyers, V. Gerginov, N. Huntemann, C. Hagemann, A. Al-Masoudi, S. Häfner, S. Vogt, U. Sterr, and C. Lisdat, *New J. Phys.* **16**, 073023 (2014).
14. T. Kessler, T. Legero, and U. Sterr, *J. Opt. Soc. Am. B* **29**, 178 (2012).
15. T. Legero, T. Kessler, and U. Sterr, *J. Opt. Soc. Am. B* **27**, 914 (2010).
16. T. Nazarova, F. Riehle, and U. Sterr, *Appl. Phys. B* **83**, 531 (2006).
17. S. A. Webster, M. Oxborrow, and P. Gill, *Phys. Rev. A* **75**, 011801(R) (2007).
18. J. Millo, D. V. Magalhães, C. Mandache, Y. Le Coq, E. M. L. English, P. G. Westergaard, J. Lodewyck, S. Bize, P. Lemonde, and G. Santarelli, *Phys. Rev. A* **79**, 053829 (2009).
19. X. Baillard, A. Gauguier, S. Bize, P. Lemonde, P. Laurent, A. Clairon, and P. Rosenbusch, *Opt. Commun.* **266**, 609 (2006).
20. M. Gilowski, C. Schubert, M. Zaiser, W. Herr, T. Wübbena, T. Wendrich, T. Müller, E. Rasel, and W. Ertmer, *Opt. Commun.* **280**, 443 (2007).
21. R. W. P. Drever, J. L. Hall, F. V. Kowalski, J. Hough, G. M. Ford, A. J. Munley, and H. Ward, *Appl. Phys. B* **31**, 97 (1983).
22. L.-S. Ma, P. Jungner, J. Ye, and J. L. Hall, *Opt. Lett.* **19**, 1777 (1994).
23. J. E. Gray and D. W. Allan, “A method for estimating the frequency stability of an individual oscillator,” in *Proceedings of the 28th Annual Symposium on Frequency Control*, Atlantic City, NJ, May 29–31, 1974 (Electronic Industries Association, 1974), pp. 243–246.
24. C. Hagemann, C. Grebing, C. Lisdat, S. Falke, T. Legero, U. Sterr, F. Riehle, M. J. Martin, and J. Ye, *Opt. Lett.* **39**, 5102 (2014).